

XPS Characterization of CeO₂ Catalyst for Hydrogenation of Benzoic Acid to Benzaldehyde

Dang-Guo Cheng · Mingben Chong ·
Fengqiu Chen · Xiaoli Zhan

Received: 27 July 2007 / Accepted: 24 August 2007 / Published online: 11 September 2007
© Springer Science+Business Media, LLC 2007

Abstract The CeO₂ catalysts for hydrogenation of benzoic acid to benzaldehyde were characterized by X-ray photoelectron spectroscopy (XPS). The results indicate the catalyst deactivation is due to the coke formation and the valence changes of Ce over the catalyst.

Keywords XPS characterization · CeO₂ · Benzaldehyde · Benzoic acid

1 Introduction

The catalytic hydrogenation of benzoic acid to benzaldehyde is a “green” technology and an alternative to current selective oxygenation of benzene [1] or toluene [2] that are characterized by low yields or not environmental friendly [1–3]. In 1988, Mitsubishi Chemicals industrialized the direct hydrogenation of aromatic carboxylic acids over modified zirconia catalysts [4]. However, ZrO₂-based catalysts in the hydrogenation of benzoic acid are not stable and produce significant amounts of by-products. Subsequently, other metal oxide catalysts, such as ZnO [5–7], Mo oxides [8–10], were also studied. Based on these reports, a typical Mars and van Krevelen mechanism is proposed in the hydrogenation of benzoic acid to benzaldehyde on metal oxides catalysts [11], as shown in Scheme 1. Therein, hydrogen activates the metal oxide by reduction to form oxygen vacancies. Then these vacancies capture the oxygen atom of carboxyl in benzoic acid and yields benzaldehyde. Therefore, the arrangement of oxygen

vacancies at the surface of the metal oxides has significant effects on catalytic behavior.

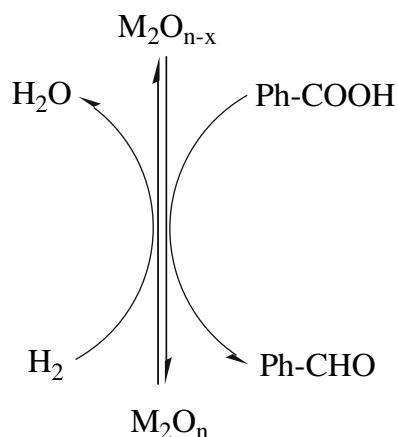
CeO₂ is one of the most interesting oxides because redox couple of Ce⁴⁺/Ce³⁺ in it can transform easily, which makes oxygen vacancies formed and eliminated rapidly [12]. It also shows good activity in hydrogenation of benzoic acid into benzaldehyde [13]. Recently, we investigated the stability of CeO₂ in hydrogenation of benzoic acid [14]. The results indicate that the CeO₂ is an effective catalyst for this reaction. However, it exhibits a little deactivation due to the coke formation primarily. Therefore, the aims of this work are to further explore the possible deactivation mechanism. By employing the X-ray photoelectron spectroscopy (XPS) the valence changes of cerium and its effect on catalytic activity in hydrogenation of benzoic acid have been investigated.

2 Experimental

2.1 Catalyst Preparation and Catalytic Measurements

The catalysts preparation was reported previously [14]. Briefly, CeO₂ catalyst was prepared by calcinating ammonium cerium nitrate (Sinopharm Chemical Reagent Co.) at 300 °C for 2 h followed by 600 °C for 4 h. The obtained sample is thus referred to Ce600. Catalyst Ce800 was prepared following the same procedure as Ce600 except that it was calcinated at 800 °C for 4 h. Catalytic measurements were carried out in a continuous flow fixed-bed reactor embedded with ca. 5 mL catalyst at atmospheric pressure, which corresponds to a GHSV of 680 h⁻¹. Ratio of H₂ to benzoic acid is 92:1 and the reaction temperature is 380 °C. Prior to reaction, the catalyst was reduced at 400 °C for 1 h. Thereafter, hydrogen flowed through a saturator containing liquid benzoic acid and both

D.-G. Cheng · M. Chong · F. Chen (✉) · X. Zhan
Department of Chemical and Biochemical Engineering,
Zhejiang University, Hangzhou, Zhejiang 310027, China
e-mail: Fqchen@zju.edu.cn



Scheme 1 The catalytic mechanism of the Ph-CHO production from Ph-COOH over metal oxide

were introduced into the reactor. To avoid condensation of benzoic acid, the connections between operation units were wrapped by heating tape and were held at a temperature of at least 250 °C. After 6-h stability test, the catalysts were regenerated in an air atmosphere at 500 °C for 4 h. Nine-regeneration and 10-stability-test cycles were conducted over the catalysts. The products were collected in an ice-cold trap at 2-h interval in each stability test and analyzed by a gas chromatography (Shimadzu GC-14B) equipped with a capillary column OV-1(30 m × 0.25 mm × 0.25 μm).

2.2 XPS Characterization

X-ray photoelectron spectroscopy (XPS) spectra for fresh, reduced, and used catalysts (i.e., nine-regeneration and 10-stability-test cycles) were recorded using a PHI1600 XPS system. A Mg K_α anode was used as the X-ray source. The binding energy of C1s (284.5 eV) was taken as internal standard for binding energy calibration.

3 Results and Discussion

The surface composition of fresh, reduced, and used (nine-regeneration and 10-stability-test cycles) catalysts is

summarized in Table 1. Using the values of surface atomic composition, an estimation of the O/Ce atomic ratio can be obtained. For fresh catalysts, either Ce600 or Ce800, it is observed that the surface oxygen concentration on the samples is higher than stoichiometric value, which is probably due to O₂ absorbed in the sample because of exposure to the atmosphere [15]. After the reduction of catalysts, the ratio increases further, which results from the formation of hydroxyl groups on the catalyst surface in the reduction with hydrogen [16, 17]. According to our previous work [14], the coke formation leads to the template deactivation of catalysts. The XPS results of used catalysts also confirm this conclusion. After the stability test, the content of carbon species increase significantly, especially for Ce800.

In the case of the ratio of lattice oxygen to cerium, the smaller of O/Ce ratio than stoichiometry, the more amounts of cerium in the Ce³⁺ state over catalysts. The results in Table 1 indicate that the reduction induces Ce⁴⁺ transformed to Ce³⁺. After the reaction, the ratio of O/Ce of Ce800 is much higher than that of Ce600. This is induced by the deep deoxygenation of benzoic acid over Ce800 which leads an increasing amount of lattice oxygen compared to bare Ce600. Therefore the yield of benzaldehyde over Ce800 is lower than that of Ce600. Shown in Table 2 is the comparison of initial activity between reduced and used (nine-regeneration and 10-stability-test cycles) catalysts. Evidently, the Ce800 exhibits a lower activity and stability in the period investigated.

Eight peaks are shown in each XPS spectrum in Fig. 1, which is in agreement with the literature reported [18]. The four main 3d_{5/2} features at 882.4, 884.9, 887.9, and 898.0 eV correspond to V, V', V'', V''' components, respectively. And the 3d_{3/2} features at 900.3, 903.5, 906.9, and 916.3 eV correspond to U, U', U'', and U''' components, respectively. The main peaks of V''' and U''' represented the 3d¹⁰4f⁰ initial electronic state corresponding to the Ce⁴⁺ ion, while a small peak of V' represented the 3d¹⁰4f¹ initial electronic state corresponding to the Ce³⁺ ion. The XP spectrum of Ce3d exhibit peaks due to the presence of both Ce⁴⁺ and Ce³⁺ over the samples.

It has been widely accepted that the relative amount of Ce⁴⁺ in CeO₂ samples can be calculated from the percent

Table 1 Surface elemental composition of CeO₂ catalysts

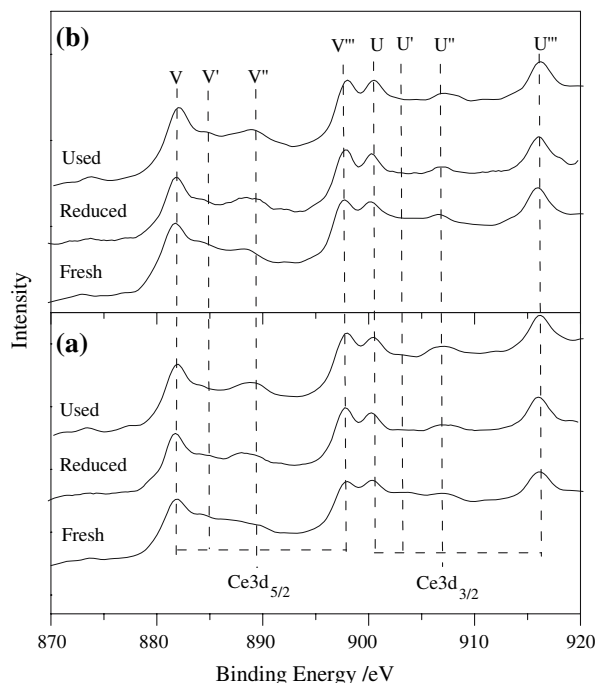
Sample		Surface composition/at %			O/Ce ^b
		C	Ce	O ^a	
Ce600	Fresh	61.5	10.6	27.9 (70.07)	2.63 (1.84)
	Reduced	61.3	10.3	28.4 (61.96)	2.76 (1.71)
	Used	72.2	7.3	20.5 (68.57)	2.81 (1.93)
Ce800	Fresh	63.6	10.0	26.4 (68.30)	2.64 (1.81)
	Reduced	66.2	8.5	25.3 (59.59)	2.97 (1.77)
	Used	81.7	4.4	13.9 (62.86)	3.15 (1.98)

^a The number in parentheses represent the atomic percentage of lattice oxygen in total oxygen content

^b The number in parentheses represent the atomic ratio of lattice oxygen to cerium

Table 2 Comparison of initial activity between reduced and used catalysts

Sample	Conversion of benzoic acid/%		Yield of benzaldehyde/%	
	Reduced	Used	Reduced	Used
Ce600	99.4	95.4	94.6	91.7
Ce800	95.1	94.3	89.9	81.0

**Fig. 1** XPS of Ce3d level for catalysts of (a) Ce600, and (b) Ce800

area of U''' peak in the total Ce3d region ($Ce\ 3d_{5/2}$ and $Ce\ 3d_{3/2}$), assuming no preferential enrichment of Ce^{4+} over Ce^{3+} or vice versa [19]. This is due to the lack of the $4f^0$ configurations in the formal Ce^{3+} state [20]. The calculated percent area of the U''' peak so defined is shown in Table 3 for the catalysts studied here. For comparison purposes, reference values for compounds containing cerium in only the Ce^{4+} or Ce^{3+} oxidation state are also given. The U''' peak for $Ce(OH)_4$ amounts to 12.4% in the Ce3d region while for $CeAlO_3/Al_2O_3$, where cerium is in the Ce^{3+} state, the U''' peak is absent [19]. Assuming a linear dependence between percent U''' and Ce^{4+} composition using the values of Table 3, the Ce^{3+} concentration over the catalysts can be estimated. For the transformation of Ce^{4+}/Ce^{3+} couple over the catalyst in the reaction, it is reasonable that the concentration of Ce^{3+} undergoes a reverse change to that of the ratio of lattice oxygen to the cerium (Table 1). The significantly lower concentration of cerium in the Ce^{3+} state observed for used Ce800 is most probably due to the deep

Table 3 Percent area of U''' peak in the total Ce 3d region ($Ce3d_{5/2}$ and $Ce3d_{3/2}$)

Sample	U''' in Ce3d/%	Ref.	Ce^{3+} concentration/at %
$Ce(OH)_4$	12.4	[19]	100
7% $CeAlO_3/Al_2O_3$	0	[19]	0
Ce600 Fresh	8.46	This work	31.78
Reduced	7.20	This work	43.94
Used	9.16	This work	26.13
Ce800 Fresh	7.97	This work	35.73
Reduced	7.61	This work	38.62
Used	9.97	This work	19.57

deoxygenation of benzoic acid, which makes the oxygen vacancy filled while Ce^{4+} is dominant over the catalyst.

4 Conclusions

In present work, the valence changes of cerium over CeO_2 catalysts for hydrogenation of benzoic acid have been investigated by XPS. The results in our experiments show that, compare to Ce600, poorer property of Ce800 could be ascribed to two reasons. The one is more coke formation on the catalysts. The other one is the valence changes of Ce over the catalyst. Because of the deep deoxygenation of benzoic acid, the transformation of the Ce^{4+}/Ce^{3+} couple over the Ce800 is unfavorable.

Acknowledgment The authors gratefully acknowledge the financial support from Science and Technology Department of Zhejiang Province, China (under contract No. 2007C21103).

References

- Zhao WJ, Jiang XZ, Zhuo GL (2005) J Mol Catal A 225:131
- Guo CC, Liu Q, Wang XT, Hu HY (2005) Appl Catal A 282:55
- Keresszegi C, Ferri D, Mallat T, Baiker A (2005) J Phys Chem B 109:958
- Van Geem PC, Janssen LHW (1988) European Patent 290096
- Hölderich WF, Tjoe J (1999) Appl Catal A 184:257
- De Lange MW, Van Ommen JG, Lefferts L (2001) Appl Catal A 220:41
- De Lange MW, Van Ommen JG, Lefferts L (2002) Appl Catal A 231:17
- Dury F, Mispion V, Gaigneaux EM (2004) Catal Today 91–92:111
- Dury F, Meixner S, Clément D, Gaigneaux EM (2005) J Mol Catal A 237:9
- Dury F, Clément D, Gaigneaux EM (2006) Catal Today 112:130
- Doornkamp C, Ponc V (2000) J Mol Catal A 162:19
- Campbell CT, Peden CHF (2005) Science 309:713
- Sakata Y, Ponc V (1998) Appl Catal A 166:173
- Chong MB, Cheng DG, Liu L, Chen FQ, Zhan XL (2007) Catal Lett 114:198

15. Zheng XC, Wang SP, Zhang SM, Wang SR, Huang WP, Wu SH (2005) *React Kinet Catal Lett* 84:29
16. Holgado JP, Alvarez R, Munuera G (2000) *Appl Surf Sci* 161:301
17. Xue L, Zhang C, He H, Teraoka Y (2007) *Appl Catal B* 75:157
18. Kondarides DI, Verykios XE (1998) *J Catal* 174:52
19. Shyu JZ, Weber WH, Gandhi HS (1988) *J Phys Chem* 92:4964
20. Creaser DA, Harisson PG, Morris MA, Wolfendale BA (1994) *Catal Lett* 13:23